

Estimating the Transmission Probability in Wireless Networks with Configuration Models

PAOLA BERMOLLEN, Facultad de Ingeniería - Universidad de la República.

MATTHIEU JONCKHEERE, Conicet - IMAS - Universidad de Buenos Aires.

FEDERICO LARROCA, Facultad de Ingeniería - Universidad de la República.

PASCAL MOYAL, Laboratoire de Mathématiques Appliquées (LMAC)-Université de Technologie de Compiègne.

We propose a new methodology to estimate the probability of successful transmissions for random access scheduling in wireless networks, in particular those using Carrier Sense Multiple Access (CSMA). Instead of focusing on spatial configurations of users, we model the interference between users as a random graph. Using configuration models for random graphs, we show how the properties of the medium access mechanism are captured by some deterministic differential equations, when the size of the graph gets large. Performance indicators such as the probability of connection of a given node can then be efficiently computed from these equations. We also perform simulations to illustrate the results on different types of random graphs. Even on spatial structures, these estimates get very accurate as soon as the variance of the interference is not negligible.

Categories and Subject Descriptors: C4 [**Computer System Organization**]: Performance of Systems—*Modelling Techniques, Performance Attributes*; G3 [**Probability and Statistics**]: Stochastic Processes

Additional Key Words and Phrases: Wireless Networks, Medium Access Probability, Random Graphs, Parking Process

1. INTRODUCTION

Wireless communications are becoming ubiquitous. Nowadays, virtually every electronic device includes at least one wireless interface. With the massive expansion of Wireless Personal Area Networks (WPAN) and Wireless Sensor Networks (WSN), and the advent of the Internet of Things (IoT), this trend will only intensify. A recent study performed by Cisco in 2011 [Evans 2011] estimated the number of devices connected to the internet per person in the world at 1.84 (if only people that are actually connected to the internet are considered, this number rises to 6.25), and that it would be 6.58 by 2020. These modern networks, decentralized and immense in size, bring along several challenges regarding performance evaluation.

In the present article, we consider a large set of nodes which communicate with each other by means of a wireless channel. In this network, a Medium Access Control (MAC) mechanism based on 802.11's Distributed Coordination Function (DCF, a form of CSMA) [IEEE 2012] is in place to allow nodes to effectively share the medium. Since every node may be either receiver or transmitter, the hidden node problem will

This work is supported by the ANII FCE-6739, CSIC ARTES group and Stic-AmSud ECHOS projects.

Author's address: P.Bermolen, Avenida Julio Herrera y Reissig 565, CP 11300, Montevideo, Uruguay, email: paola@fing.edu.uy; M. Jonckheere, (1428) Pabellón I, Ciudad Universitaria Buenos Aires, Argentina, email: mjonckhe@dm.uba.ar; F.Larroca, Avenida Julio Herrera y Reissig 565, CP 11300, Montevideo, Uruguay, email: flarroca@fing.edu.uy; P.Moyal, Rue Roger Couttolenc, CS 60319, 60203 Compiègne Cedex, France, email: pascal.moyal@utc.fr

Permission to make digital or hard copies of all or part of this work for personal or classroom use is granted without fee provided that copies are not made or distributed for profit or commercial advantage and that copies bear this notice and the full citation on the first page. Copyrights for components of this work owned by others than ACM must be honored. Abstracting with credit is permitted. To copy otherwise, or republish, to post on servers or to redistribute to lists, requires prior specific permission and/or a fee. Request permissions from permissions@acm.org.

© 2015 ACM. 2376-3639/2015/12-ARTXXXX \$15.00

DOI: <http://dx.doi.org/10.1145/2858795>

probably degrade the network's performance if unattended [Larroca and Rodríguez 2014]. The typical way of dealing with this problem is to use the RTS/CTS four-way handshake.

With this mechanism in place, every node that intends to send a packet to a tagged destination first senses the medium, and if idle, it sends a Ready To Send (RTS) frame addressed to it. This packet contains the duration of the impending transmission, so all nodes overhearing the packet will refrain from transmitting during this period. If possible, the destination node will in turn respond with a Clear To Send (CTS) frame, which also contains the duration, and thus every other node overhearing this frame will also restrain itself from transmitting. However, if the tagged destination has previously overheard another CTS frame, or its channel is currently not idle, it will naturally not answer the RTS, and the transmission will not take place.

We are interested in the transmission probability, that is the number of concurrent *successful* transmissions that take place in such a network (which is also termed as the spatial reuse in the literature). In particular, we consider a slotted variant of DCF. That is to say, time is broken into slots of duration T_s , which in turn are separated in two periods: the so-called contention period (T_c) and the transmission period (T_t). During the first one, all nodes that have a packet ready to be sent choose a random time between 0 and T_c , when they send an RTS frame to the destination node. Naturally, this will happen unless they sensed the medium as busy or they overheard another RTS or CTS frame first. The destination node will in turn answer with a CTS frame unless its medium is currently busy, or if it received another RTS or CTS frame first. After the RTS/CTS handshake successfully took place, the data packet is sent immediately.

Before stating our contributions in more detail, a brief state of the art on wireless networks driven by access control mechanisms is in order. The dynamics induced by randomized decentralized medium access protocols have received a tremendous amount of attention, due on the one hand to their dominant deployment, and on the other hand to the great difficulty of their modeling and performance evaluation. Even the simplest algorithms where users do not use any information on the contents of their own or their neighbors buffers to access the channel are far from understood. A realistic model should indeed combine at least the two following interacting sources of randomness:

- (1) Randomness of the media: interference between users competing for communication (that may depend on the stochastic spatial positions of users as well as on various sources of noise).
- (2) Randomness of the traffic: stochastic arrivals and departures of users.

Moreover, users can be considered saturated (they always have packets to transmit) or unsaturated (i.e., each user represents an exogenous source of traffic for the network), while traffic can be modeled as asymmetric and subject to priority mechanisms (tree-algorithms). These difficulties gave rise to different types of models focusing on specific aspects and sources of randomness:

- A first class of models does not take into account the spatial diversity and considers scenarios where every user symmetrically interacts with everyone else. Some authors use the term full interference to describe this situation which might be a very pessimistic assumption. (In that context for instance, the non-adaptive ALOHA can be shown to be unstable for almost any traffic parameter [Bremaud 1999].) More accurate models may however focus on possible asymmetric and dynamical stochastic traffic characteristics. This line of research started with the seminal work of Bianchi [Bianchi 2000].

- Another family of models focuses on a fixed graph of interference with unsaturated users. In this context, the first benchmark of performance is to characterize the stability of the network which might turn out to be a difficult task. Under Markovian assumptions, a characterization of the stability problems has been obtained in [Szpankowski 1983; Borst et al. 2008]. More detailed characterizations and approximations of the stability region were recently obtained in [Cecchi et al. 2014], while it was shown in [Bordenave et al. 2012] how to approximate the stability region using mean-field arguments.
- On the other side of the spectrum, some models inspired by stochastic geometry and point processes focus on the random spatial location of users and aim at estimating e.g. the probability of connections for a given users' configuration. A pioneering application of Matérn's model can be found in [Nguyen et al. 2007] while more involved models and computations are considered in [Baccelli and Blaszczyzyn 2009a; 2009b]. Since a partial interference (not all users interfere between each other) is an important feature of wireless networks, it is crucial to grasp its quantitative influence on performance. To further take into account the stochastic nature of traffic, a time scale separation assumption might then be called upon to use the probability of access in a given state of the system as the speed of service of a higher time scale stochastic network.

This last point of view is close to the one we adopt here. However, the evaluation of connection probabilities for a given scenario remains a difficult task. This is linked to the analysis of the dynamics of the so-called parking process, which has received a tremendous amount of attention in the physics and biology literature (under the name of random adsorption models) [Penrose 2001; Penrose and Sudbury 2005]. Even in the case of completely symmetric users, evaluating the probability of connection when users are spatially located as a Poisson point process in the plane is a difficult problem.

Recently, a characterization of the Laplace transforms of functionals of the parking process dynamics (also called the Matérn-infinity process) were obtained [Viet and Baccelli 2012b; 2012a]. These are striking results given the complexity of the process. Unfortunately they do not provide explicit formulas for the probability of a successful transmission for instance and bounds have to be invoked to obtain easily computable estimates. Moreover, nodes competing to access the channel in these models may only transmit. After the decision of which nodes may do so simultaneously, the receiver is considered as any point at distance less than a given threshold, and the coverage probability is analyzed (i.e. the context is more adequate for downlink transmissions where the nodes that compete to access the channel do not communicate between them, and the RTS/CTS handshake is not considered). On the contrary, in our work all nodes may be either transmitter or receiver, and the receiver's availability is also considered to establish the transmission.

Naturally, some efforts have been carried out in order to consider the receiver. Most notably, in [Durvy and Thiran 2006] a packing approach of links is considered to calculate the spatial reuse in slotted medium access control of multi-hop ad-hoc networks. However, with the proposed methodology an explicit formula for the spatial reuse may be obtained for the line topology only, whereas for the grid or Poisson distribution on the plane they based their analysis on simulations. The method we propose here may be used for any topology and in particular, as we will see on the example section, provides an asymptotically exact approximation for the line topology.

We hence take here an alternative route. Building on some recent results for parking processes on random graphs, we base our estimation of connection probabilities on dynamics over random graphs rather than on thinned point processes. Just as models inspired by stochastic geometry, we consider a single time slot but we forget the spatial

configurations of users to focus on a random graph of interference. Though this method might lose in accuracy by ignoring some correlations between users interferences, it allows to get simple differential equations through which one can easily compute the probability of connection.

More specifically, we provide a methodology that allows us to calculate the probability of a successful transmission in an arbitrarily large random network, where a CSMA-like protocol is in place and the RTS/CTS handshake is active. This is our main contribution and is achieved by constructing jointly the interference graph and an associated exploration process, permitting us to define the dynamics of the parking process as a measure-valued Markov process. Then by means of classical martingale decomposition of Markov process, we show how the dynamics of the process can be described by a system of non-linear differential equations when the size of the graph is large.

The structure of the paper is as follows. After stating our assumptions in the next section, we describe the parking process on a fixed graph in Sec. 3 and motivate the need of defining simultaneously the graph and the dynamics. In the same section, we provide an intuitive description of the definition of the measure-value Markov process and the large graph limit. Our main result is presented and explained in Sec. 4. This result is obtained by using and extending our previous work [Bermolen et al. 2013] which may be regarded as an analysis where the receiver node is not considered. Finally, in Sec. 6 we will show how to analyze variants of the access mechanism, which differ in how the transmitter (and the overhearing nodes) reacts to a failed handshake. Moreover, the usefulness of the presented results is illustrated by studying several example scenarios (Sec. 5).

2. CONTEXT AND ASSUMPTIONS

We assume in the sequel a threshold-type channel, where transmissions are either perfectly received or not received at all. This is sometimes termed *protocol model* in the literature [Gupta and Kumar 2000]. In other words, we consider an interference graph $\mathcal{G} = (\mathcal{V}, \mathcal{E})$, where an edge exists from node s to node r if the transmission of node s can be received by node r . We further assume that the channel is symmetric, meaning that all edges are bidirectional. Practically speaking, this means that all wireless nodes have relatively similar hardware and transmit at the same power. The last assumption is that the RTS/CTS handshake takes place instantly. This means that thanks to the collision avoidance scheduling, no collisions will occur in our model.

Let us now discuss how to model the communication graph. In a planned network, where all nodes are fixed and the propagation conditions are stable, the graph is given and does not change significantly over time. This could be the case in a wireless mesh with line-of-sight between nodes. However, if nodes are mobile and/or the channel rapidly changes (for instance, a MANET or a urban scenario), the graph may vary significantly, thus adding a second level of randomness (that is, in addition to the MAC layer). We focus on the second scenario, although we will later discuss how our results may be used in the static case-scenario.

Consider for instance the “most random” graph possible: a scenario where every pair of nodes are neighbors (i.e. an edge exists between them) with probability p , and the event of two nodes being neighbors is independent of everything else. This graph models a totally unplanned and dynamic network, where all we may be able to estimate a priori is p . In particular, let us denote by N the total number of nodes in the network, and by ν the average number of neighbors of each node. Then, $p(N - 1) = \nu$, and if N is big, this amounts to $p \approx p_N = \nu/N$. Thus, the parameter of interest in this scenario is ν .

We may however have more information on the communication graph than the mean number of neighbors. In particular, we assume here that the graph of interference is characterized by the complete distribution of degrees denoted h_N . For example, we may know that half the nodes have two neighbors, and the other half three, in which case the counting measures of degrees is such that $h_N(2) = h_N(3) = 1/2$, and 0 for the rest. For the example described in the previous paragraph the degree distribution is $h_N(i) = C_i^{N-1} p^i (1-p)^{N-1-i}$ (i.e. a binomial distribution), which may be approximated by a Poisson distribution with parameter ν when N is large.

Regarding traffic, we assume that all nodes are saturated i.e. have a packet ready to be sent in every time-slot. We further assume that the destination node for this packet is a neighbor picked at random. Let us consider a given contention period. At time 0, every node will choose a random number, uniformly distributed between 0 and T_c . Consider the node with the minimum such time. It will send a RTS frame to one of its neighbors, chosen randomly among them. Since this is the first transmission, the destination node will answer with a CTS frame, thus “blocking” all its neighbors. The origin node will immediately start transmitting a data frame, also blocking all its neighbors. In what follows, we will term these two nodes as *active*, and their neighbors as *blocked*. Just like the receiving node, blocked nodes stop competing for the channel. Let us term the rest of the nodes as *unexplored*.

We now have to focus solely on this last set, and find the node which has drawn the minimum number. This node will then send a RTS frame to any of its neighbors. However, the receiving node may already be blocked by a previous transmission and/or CTS, in which case the handshake will fail. As a first step in the analysis, and in the following two sections, we will assume that the origin node realizes this failure (since no CTS is received), and immediately sends a new RTS frame to another random neighbor. This is repeated until a CTS is received back, or no more neighbors are left (i.e. all its neighbors belong to the blocked set). Furthermore, the transmission of the RTS frames will also be assumed to take place instantly. In addition to allowing us to illustrate the techniques we will use in the analysis, this scenario is of interest on its own right, since it models an ideal protocol and may be regarded as an upper bound for the resulting probability of successful transmission.

Finally, the above procedure is repeated until time T_c , or equivalently, until no more unexplored nodes are left.

3. PRELIMINARIES

3.1. Random sequential adsorption

We now start the analysis with the objective of estimating the number of successful transmissions that take place concurrently. That is to say, how many CTS frames are sent in a single time slot on average. The first step will be to construct the interference graph $\mathcal{G} = (\mathcal{V}, \mathcal{E})$. Since our only a priori information is the nodes’ degree distribution $h_N(i)$, we will consider a uniformly chosen graph among those that comply with it.

Having chosen a graph, we proceed to analyze the MAC protocol. Please recall that each node chooses a random time (uniformly drawn from the interval $[0, T_c]$) to send its RTS frame. However, regarding the order at which they will proceed, which ultimately determines the successful transmissions that will take place, any other continuous distribution is equivalent. In particular, the exponential distribution with parameter λ is one that will serve our purposes (with λ any positive number). Let us now denote by \mathcal{U}_t , \mathcal{A}_t and \mathcal{B}_t the set of unexplored, active and blocked nodes at time t respectively (with $\mathcal{U}_t \cup \mathcal{A}_t \cup \mathcal{B}_t = \{1, \dots, N\} \forall t$). At time 0 we have $\mathcal{A}_0 = \mathcal{B}_0 = \emptyset$ and $\mathcal{U}_0 = \{1, \dots, N\}$.

Please note that, given \mathcal{G} , the triplet $(\mathcal{U}_t, \mathcal{A}_t, \mathcal{B}_t)$ forms a non-homogeneous continuous time Markov chain. Transitions updating the sets \mathcal{U}_t , \mathcal{A}_t and \mathcal{B}_t occur when RTS

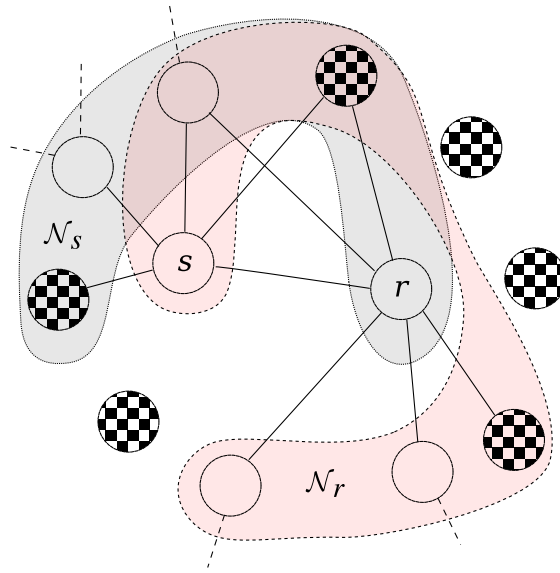


Fig. 1. An example of \mathcal{N}_s and \mathcal{N}_r when a r in $\mathcal{U}_{t_n}^+$ exists. Nodes with no fill were unexplored at time t_n . Only the connections of s and r are shown.

frames are transmitted, and since only unexplored nodes compete for the channel, their rate is equal to $|\mathcal{U}_t| \lambda$. For instance, in our present ideal scenario, a RTS transmission will be successful if the tagged node has at least one unexplored neighbor. Figure 1 illustrates an example of such a transition, where node s sends a RTS to node r (a random node from its unexplored neighbors). Thus, both will be transferred from \mathcal{U}_t to \mathcal{A}_t , and all nodes in \mathcal{N}_s and \mathcal{N}_r (their neighbors) will now belong to \mathcal{B}_t (or more precisely, except r and s , those which were not blocked already). This is repeated until transition time t_{n^*} , when $\mathcal{U}_{t_{n^*}} = \emptyset$, an absorbing state of this Markov chain.

The algorithm described above belongs to the class of the so-called *Parking Processes* [Penrose 2001]. In this context, the set $\mathcal{A}_{t_{n^*}}$ is termed *Jamming limit*, and is related to our ultimate objective: to estimate the number of successful transmissions in a typical contention period. To this end, one may try to study the Markov chain on a fixed graph, calculate the Jamming limit given a particular communication graph \mathcal{G} , and then combine these results weighting them by the probability of every particular graph. Unfortunately, this brute-force approach will quickly be limited by the immense size of the state space of the Markov chain. This explains the need for an alternative, more tractable, approach.

3.2. Configuration algorithm and measure-valued Markov process for large graphs

Given the difficulties emphasized above, our approach consists in constructing the random graph \mathcal{G} jointly with the transmissions' dynamics, following the so-called configuration model [Bollobas 2001; Molloy and Reed 1995; Durrett 2007]. In this first approach, the construction focuses only on the unexplored nodes. In fact, we are interested in how many CTSs have been sent by the time the unexplored set \mathcal{U}_t becomes empty.

To this end, let us recall that at any time t , a node can be an element of either \mathcal{U}_t , \mathcal{A}_t or \mathcal{B}_t . Moreover, our only a priori information is the counting measure μ , where $\mu(i)$ is the number of unexplored nodes having i unexplored neighbors at time 0 (i.e.,

$\mu(i) = h_N(i)N \forall i \in \mathbb{N}$). We then extend this to an arbitrary time $t > 0$ and denote it as μ_t .

It is important to highlight that we do **not** require the knowledge of which particular nodes are the neighbors of any given unexplored node. As such, we regard the edges starting from any node in \mathcal{U}_t as *unmatched* half-edges from an unexplored node towards either another unexplored node (and we denote them as $U \rightarrow U$) or a blocked node (which will naturally be denoted by $U \rightarrow B$). In this sense, $\mu_t(i)$ tells us how many unexplored nodes have i half-edges of class $U \rightarrow U$ at time t . As we now discuss, by characterizing μ_t alone we will be able to estimate the transmission probability.

Let us denote for all $t \geq 0$ and all $i \in \mathbb{N}$,

$$\alpha_t(i) = \frac{\mu_t(i)}{\sum_{j \in \mathbb{N}} \mu_t(j)}; \quad (1)$$

$$\beta_t(i) = \frac{i\mu_t(i)}{\sum_{j \in \mathbb{N}} j\mu_t(j)}. \quad (2)$$

The probability measures α_t et β_t have intuitive interpretations: the first one describes the degree distributions of a randomly (and uniformly) picked unexplored node at time t , while the second one is the size biased distribution of α_t and represents the degree distribution of any neighbor of a randomly picked unexplored node or in other words, the degree of the starting node of a half-edge drawn uniformly at random, among all half-edges starting from unexplored nodes. This representation will be useful in the following discussion.

Suppose that at a transition time t_n , a formerly unexplored node transmits a RTS frame, thus becoming active. Let us term this node as TX. Then, the measure μ_{t_n} has to be modified according to the following steps:

- (1) TX is chosen uniformly among all unexplored nodes. We shall denote by K^{TX} **its degree towards other unexplored nodes**. Hence,

$$P(K^{\text{TX}} = i) = \alpha_{t_n}(i), i \in \mathbb{N}. \quad (3)$$

(Note that we have dropped the dependence on time for K^{TX} to lighten notations and we shall do the same for other quantities of interest in the sequel.)

Then, as TX becomes active and is no longer unexplored, we have to remove it from the measure μ_{t_n} : the quantity $\mu_{t_n}(i)$ is decreased by one in $i = k^{\text{TX}}$, a particular realization of K^{TX} (for example $k^{\text{TX}} = 3$ in Fig. 1). If $k^{\text{TX}} = 0$, then this transmission attempt will fail and we proceed to the next transmission attempt, if any.

- (2) If $k^{\text{TX}} > 0$, we complete the edges starting from TX using a uniform pairing procedure, as termed in [Wormald 1995]: each one of the k^{TX} half-edges emanating from TX is matched with another half-edge, drawn uniformly at random among all available ones. By doing so, two ‘bad’ situations may occur:
 - (2a) half-edges emanating from TX are matched together, creating self-loops;
 - (2b) several half-edges of TX are matched to half-edges emanating from the same node, hence generating multiple edges between TX and the latter.

However, the probability of such events for a fixed TX becomes arbitrarily small as N grows large. Indeed, one can show that similarly to Formulas (54) and (56) in [Bermolen et al. 2013] (for the system without receiver), as long as the quantity of remaining half-edges remains of order N , the probability that TX has self-loops and/or multiple edges is of order $1/N$. As an alternative argument, one can observe that the uniform construction of the random graph leads to the configuration model (see [Wormald 1999], independence property), for which the number of self-loops (case 2a) and multiple edges (2b) tends in distribution to a Poisson random variable

whose parameter is independent of N (see *e.g.* Proposition 7.9 in [van der Hofstad 2013]), hence to an arbitrarily small quantity with respect to N .

As a conclusion, up to this asymptotically negligible events, TX shares its k^{TX} edges with k^{TX} other nodes. At this point, one of these unexplored neighbors of TX also becomes active: this node is denoted by RX, the intended destination of TX's RTS.

If $k^{\text{TX}} > 1$, we also need to block all the unexplored neighbors of TX except RX, and for this we repeat the same random matching procedure $k^{\text{TX}} - 1$ times. In total, there are exactly k^{TX} U-nodes changing status at this stage (the new RX and the other neighbors of TX), and we have to know their respective degrees to update the measure accordingly. Observe that at t_n , precisely $i\mu_{t_n}(i)$ half-edges belong to a node that has a degree i towards unexplored nodes. Let for any i , $Y^{\text{TX}}(i)$ be the number of neighbors of TX (including RX) having degree i toward the unexplored vertices just before t_n . In view of the previous observation, conditionally on K^{TX} , $Y^{\text{TX}}(i)$ is a hypergeometric random variable with parameters k^{TX} and $\beta_{t_n}(i)$. All in all, for any i , $\mu_{t_n}(i)$ decreases by the quantity $y^{\text{TX}}(i)$, a realization of $Y^{\text{TX}}(i)$ (for example $y^{\text{TX}}(3) = 2$, $y^{\text{TX}}(4) = 1$, and $y^{\text{TX}}(i) = 0 \forall i \neq 3, 4$ in Fig. 1).

- (3) Let us denote by K^{RX} , the **number of unmatched** $U \rightarrow U$ **half-edges starting from** RX (for example, $k^{\text{RX}} = 4$ in Fig. 1). Set $K^{\text{RX}} \equiv 0$ if $k^{\text{TX}} = 0$. As the random pairing is uniform, conditionally on $\{K^{\text{TX}} > 0\}$ the distribution of the r.v. K^{RX} is given by

$$P(K^{\text{RX}} = i) = \beta_{t_n}(i), i \in \mathbb{N}^*. \quad (4)$$

Likewise the previous step, if $k^{\text{RX}} > 1$, we now have to block all the unexplored neighbors of RX, except TX and all its (already blocked) neighbors. Let $Y^{\text{RX}}(i)$ be the number of such neighbors of RX, having degree i toward the unexplored vertices at t_n . The distribution of the latter r.v. depends on the number of neighbors that TX and RX have in common. Such neighbors may very well exist, as the example in Fig. 1 illustrates. But using a similar argument as for the case (2a) above, in the large graph limit, the probability of RX choosing one (or more) of the neighbors of TX is arbitrarily small, until any given horizon strictly prior to the completion of the graph (in which case the sum of the degrees of the neighbors of TX remains negligible with respect to the total choice of half-edges proposed to RX - similarly to the convergence of the first term in Lemma 5.1 of [Bermolen et al. 2013]). All the same, the probability that RX has self-loops, or shares multiple edges with its neighbors tends to 0 as N grows large (as in (2b)). Therefore, in the limit, $Y^{\text{RX}}(i)$ is a hypergeometric random variable with parameters $k^{\text{RX}} - 1$ and $\beta_{t_n}(i)$. As above, for any i , $\mu_{t_n}(i)$ additionally decreases by the quantity $y^{\text{RX}}(i)$ (in the example of Fig. 1 $y^{\text{RX}}(2) = 2$ and $y^{\text{RX}}(i) = 0 \forall i \neq 2$).

- (4) Once we have blocked all the neighbors of both TX and RX, all their formerly $U \rightarrow U$ half-edges become either $B \rightarrow A$ (the ones pointing towards either TX or RX) or $B \rightarrow U$ (all the other ones, see the slashed edges in Fig. 1). Consequently, the same number of $U \rightarrow U$ half-edges emanating from unexplored nodes now become $U \rightarrow B$, thereby creating edges between blocked and unexplored nodes. More precisely, each blocked node completes its former $U \rightarrow U$ half-edges with any of the available ones, uniformly chosen at random. The discussion regarding the case (2b) above still applies: as N goes to infinity the probability of choosing (i) a half-edge belonging to another blocked neighbor (hence creating edges between blocked nodes), or (ii) several half-edges emanating from the same unexplored node (leading to multiple edges), vanishes as N grows large. (In the example in Fig. 1, five unexplored nodes will "lose" one $U \rightarrow U$ half-edge, as each of the five slashed half-edges point towards a different node.)

Hence, in terms of the random vectors defined before, and whenever $K^{\text{TX}} > 0$, there are $Z^{\text{TX}} = \sum_{\ell > 0} (\ell - 1) \left(Y^{\text{TX}}(\ell) - \mathbb{1}_{\{K^{\text{RX}} = \ell\}} \right)$ (respectively, $Z^{\text{RX}} = \sum_{\ell > 0} (\ell - 1) Y^{\text{RX}}(\ell)$) unexplored nodes neighboring the blocked neighbors of TX (resp., of RX) that lose one $U \rightarrow U$ half-edge (in the example of Fig. 1 $z^{\text{TX}} + z^{\text{RX}} = 5$). Let us define for all i , $X^{\text{TX}}(i)$ (resp., $X^{\text{RX}}(i)$) the r.v. indicating **how many such nodes have a degree i towards the unexplored nodes**. The latter is hypergeometric with parameters Z^{TX} (resp., Z^{RX}) and $\beta_{t_n}(i)$. Using these definitions, in this last step, for any i , $\mu_{t_n}(i)$ decreases by $x^{\text{TX}}(i) + x^{\text{RX}}(i)$ and increases by $x^{\text{TX}}(i + 1) + x^{\text{RX}}(i + 1)$.

The above description shows that (μ_t) is a measure-valued continuous-time inhomogeneous Markov chain (see [D.A. 1991]), admitting the null measure $\mathbf{0}$ as absorbing state.

Let us further add another dimension to the process and additionally keep track, for all t , of the number c_t of CTS frames that have been sent up to time t . It is easily seen that (μ_t, c_t) is still a Markov chain. We are thus interested in c_t after the chain reaches an absorbing state, considering that the following equality holds:

$$\mathbb{E}\{\Theta\} = \theta = \lim_{t \rightarrow \infty} \mathbb{E} \left\{ \frac{c_t}{N} \right\},$$

where Θ is a random variable indicating the number of successful transmissions obtained in a given contention period, divided by the total number of nodes (N). The next section shows how the limit above may be obtained by characterizing the dynamics of μ_t .

4. LARGE GRAPH LIMIT

As we discussed in the previous section, the probability of a successful transmission can be described as a function of the Markov process (μ_t, c_t) . Though computations on the defined Markov chain are still a formidable task for large state spaces, the system dynamics get simpler to understand for large N . In fact, c_t can be expressed in the limit by means of a differential equation (where naturally μ_t plays a central role).

Let us emphasize the dependence of the measure-valued process on the size N of the graph by denoting the latter (μ_t^N) . As N grows large, we consider a scaled process $(\bar{\mu}_t^N) := (\mu_t^N / N)$ (thus for all i , $\bar{\mu}_t^N(i)$ refers to the proportion of unexplored nodes with i unexplored neighbors at time t for the graph of size N). We then identify the so-called large-graph limit $\bar{\mu}$ by letting N go to infinity, thereby obtaining a functional law of large numbers for the system. This limiting process gives us a representation of the “mean behavior” of the measure valued process (μ_t) , and performance indicators as a by-product.

In what follows, for any t , for any fixed measure $\bar{\mu}_t$ we denote likewise (1) and (2),

$$\bar{\alpha}_t(i) = \frac{\bar{\mu}_t(i)}{\sum_{j \in \mathbb{N}} \bar{\mu}_t(j)}; \quad (5)$$

$$\bar{\beta}_t(i) = \frac{i \bar{\mu}_t(i)}{\sum_{j \in \mathbb{N}} j \bar{\mu}_t(j)}. \quad (6)$$

The following result can be seen as an extension of Theorem 4.1 in [Bermolen et al. 2013], which establishes a similar large-graph limit for a measure-valued process representing an ideal system, in which only the neighbors of TX are blocked. In particular, we have to make similar mild assumptions on the initial conditions of the system.

ASSUMPTION 4.1. *Let for any $k \geq 0$, χ^k denote the function $x \rightarrow x^k$ and $\langle \mu, \phi \rangle = \sum_i \mu(i)\phi(i)$. For all bounded functions ϕ from \mathbb{N} to itself,*

$$\langle \bar{\mu}_0^N, \phi \rangle \xrightarrow{N \rightarrow \infty} \langle \nu, \phi \rangle \text{ in probability,} \quad (7)$$

where ν is a deterministic finite measure on \mathbb{N} such that

$$0 < \langle \nu, \chi \rangle \text{ and } \langle \nu, \chi^6 \rangle < \infty. \quad (8)$$

We then have the following result.

THEOREM 4.2. *Under Assumption 4.1, the sequence of processes $\{\bar{\mu}^N\}$ converges in probability and uniformly on compact time intervals towards the only measure-valued deterministic function $\bar{\mu}$ of the following infinite dimensional differential system: for all $t \geq 0$ and all $i \in \mathbb{N}$,*

$$\begin{aligned} \bar{\mu}_0(i) &= \nu(i); \\ \frac{d}{dt} \bar{\mu}_t(i) &= -\lambda \sum_{\ell} \bar{\mu}_t(\ell) \left[\bar{\alpha}_t(i) + \bar{\beta}_t(i) \left(\sum_j j \bar{\alpha}_t(j) + (1 - \bar{\alpha}_t(0)) \sum_j (j-1) \bar{\beta}_t(j) \right) \right. \\ &\quad \left. + \left(\bar{\beta}_t(i) - \bar{\beta}_t(i+1) \right) \sum_j (j-1) \bar{\beta}_t(j) \right] \left(\sum_j j \bar{\alpha}_t(j) + (1 - \bar{\alpha}_t(0)) \sum_j (j-2) \bar{\beta}_t(j) \right) \right]. \end{aligned} \quad (9)$$

PROOF. The mathematical steps leading to this fluid limit result are standard in the theory of weak approximations of Markov processes. They can be obtained similarly to Theorem 4.1 of [Bermolen et al. 2013], and are not further described in detail. In a few words, one first considers the process until an instant t_ε arbitrarily close, but strictly less than the completion time of the graph, so that the large-graph approximation of Sec. 3.2 remains valid. Then, until t_ε , classical martingale arguments entail that the only limit point $\bar{\mu}$ of $(\bar{\mu}^N)$ is the (unique) deterministic flow satisfying for any test function $\mu \mapsto \mu(i)$, $i \in \mathbb{N}$, the ordinary differential equation

$$\frac{d\bar{\mu}_t(i)}{dt} = F_t(i)(\bar{\mu}),$$

where the drift $F_t(i)$ is nothing but the limiting expected value of the decay of $\frac{\mu_t^N(i)}{N}$. That is to say, the mean number of nodes with i half-edges of type $U \rightarrow U$ that are removed at t if a transition occurs at that time, times the normalized transition rate. In other words, for all i ,

$$\begin{aligned} \frac{d}{dt} \bar{\mu}_t(i) &= -\lambda \sum_{\ell} \bar{\mu}_t(\ell) \left[\bar{\alpha}_t(i) + P(K^{\text{TX}} > 0) \mathbb{E} \{ Y^{\text{TX}}(i) + X^{\text{TX}}(i) - X^{\text{TX}}(i+1) | K^{\text{TX}} > 0 \} \right. \\ &\quad \left. + P(K^{\text{TX}} > 0) (\mathbb{E} \{ Y^{\text{RX}}(i) \} + \mathbb{E} \{ X^{\text{RX}}(i) - X^{\text{RX}}(i+1) \}) \right]. \end{aligned} \quad (10)$$

In the right hand side of (10), the first term between brackets corresponds to the transmitter node. If $K^{\text{TX}} > 0$, then additional nodes of degree i may be blocked both by TX and RX, which correspond to the last terms.

Now, according to the large-graph asymptotics discussed in Section 3.2, the limiting expected valued of the involved random variables are given by

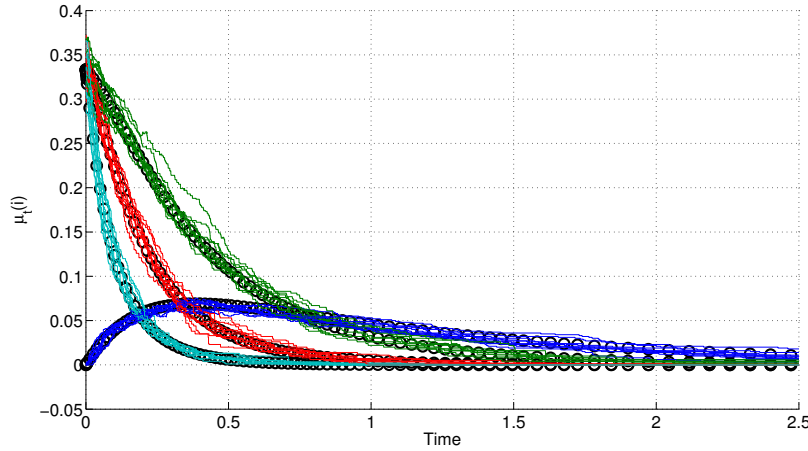


Fig. 2. An example comparing several realizations of $\bar{\mu}_t^N$ ($N = 1000$) and the solution of (9) (marked as circles), where $\bar{\mu}_0^N = \bar{\mu}_0 = (0, 1/3, 1/3, 1/3)$. The four coordinates of the process are shown superposed.

$$\begin{aligned} \mathbb{E}\{Y^{\text{TX}}(i)|K^{\text{TX}} > 0\} &= \bar{\beta}_t(i)\mathbb{E}\{K^{\text{TX}}|K^{\text{TX}} > 0\} = \bar{\beta}_t(i)\frac{1}{1-\bar{\alpha}_t(0)}\sum_j j\bar{\alpha}_t(j); \\ \mathbb{E}\{X^{\text{TX}}(i)|K^{\text{TX}} > 0\} &= \bar{\beta}_t(i)\mathbb{E}\{Z^{\text{TX}}|K^{\text{TX}} > 0\} = \bar{\beta}_t(i)\sum_{\ell>0}(\ell-1)\mathbb{E}\{Y^{\text{TX}}(\ell) - \mathbb{1}_{\{K^{\text{RX}}=\ell\}}|K^{\text{TX}} > 0\} \\ &= \bar{\beta}_t(i)\sum_l(l-1)\bar{\beta}_t(l)\sum_j j\frac{\bar{\alpha}_t(j)}{1-\bar{\alpha}_t(0)} - \bar{\beta}_t(i)\sum_l(l-1)\bar{\beta}_t(l); \\ \mathbb{E}\{Y^{\text{RX}}(i)\} &= \bar{\beta}_t(i)\mathbb{E}\{(K^{\text{RX}} - 1)\} = \bar{\beta}_t(i)\sum_j(j-1)\bar{\beta}_t(j); \\ \mathbb{E}\{X^{\text{RX}}(i)\} &= \bar{\beta}_t(i)\sum_{\ell>0}(\ell-1)\mathbb{E}\{Y^{\text{RX}}(\ell)\} = \bar{\beta}_t(i)\sum_l(l-1)\bar{\beta}_t(l)\sum_j(j-1)\bar{\beta}_t(j). \end{aligned}$$

Then (9) follows by straightforward algebra. The convergence result after t_ε can be obtained similarly to Lemma 5.6 in [Bermolen et al. 2013]. ■

Example 4.3.

Before discussing how to calculate the probability of connection, let us consider an example. In particular, assume a large network where all we know is that nodes may have either 1, 2 or 3 neighbors with the same probability. In this case, $\bar{\mu}_0^N(i) = 1/3$ for $i = 1, 2, 3$, and $\bar{\mu}_0^N(i) = 0$ for the rest. It is then straightforward to see that in this case the infinite dimensional differential equation described by Eq. (9) results in a 4-dimensional one, where we have to determine $\bar{\mu}_t(i)$ for $i = 0, \dots, 3$, and the rest will be identically zero. In general, if $\bar{\mu}_0(i) = 0$ for all $i > D$, then the system has $D + 1$ differential equations with $D + 1$ functions to be calculated. In this case, we may resort to numerical methods to solve the system.

The resulting solution $\bar{\mu}_t$ and several realizations of $\bar{\mu}_t^N$ (with $N = 1000$) for this particular example are compared in Fig. 2. The graph illustrates how $\bar{\mu}_t$ effectively represents the “mean” of the actual process $\bar{\mu}_t^N$.

4.1. Estimating the probability of successful transmission

Let us now discuss how to calculate the transmission probability based on $\bar{\mu}_t$. As discussed before, we may define an auxiliary Markov process (c_t) , that counts for any time t , how many CTS frames have been sent up to time t . Its transition times are the same as that of (μ_t) , and it will increase by one at t only if a CTS is received by the tagged node (i.e. if it has an unexplored neighbor) which occurs with probability $1 - \alpha_t(0) = 1 - \mu_t(0) / \sum_j \mu_t(j)$. Based on the previous result, the process (c_t/N) converges when N goes to infinity, in the same sense as above, to the deterministic function (\bar{c}_t) which is defined by

$$\frac{d}{dt} \bar{c}_t = \lambda \sum_j \bar{\mu}_t(j) \left(1 - \frac{\bar{\mu}_t(0)}{\sum_j \bar{\mu}_t(j)} \right) = \lambda \sum_{j>0} \bar{\mu}_t(j); t \geq 0,$$

where $\bar{\mu}$ is the only solution of (9). Since the transmission probability is simply the limit of (\bar{c}_t) for large t , we have obtained the following result:

PROPOSITION 4.4. *Let Θ be a random variable indicating the proportion of successful transmissions that take place in a given contention period, as described in Secs. 3.1 and 3.2. When N goes to infinity the following equality holds:*

$$\mathbb{E}\{\Theta\} = \theta = \lambda \int_0^\infty \sum_{j>0} \bar{\mu}_t(j) dt, \quad (11)$$

where $(\bar{\mu}_t)$ is the only solution of (9).

Please note that although Th. 4.2 proves the convergence on a compact interval (until just before the graph's completion time), Eq. (11) remains valid. Firstly, the solution of (9) can be extended to \mathbb{R}^+ by continuity arguments, similarly to the comment before Lemma 5.6 in [Bermolen et al. 2013] and secondly, its integral after the completion time can be proved to be negligible, as in the proof of Corollary 4.4 in [ibid.].

Remark 4.5. As expected, the value of $\theta = \int_0^\infty \sum_{j>0} \bar{\mu}_{t/\lambda}(j) dt$ does not depend on λ . From (9), we obtain that the function $\mu_{t/\lambda}(i)$ verifies an ordinary differential equation of the form $\frac{d}{dt} \mu_{t/\lambda}(i) = F(\mu_{t/\lambda}(i))$ where F does not depend on λ . Then, the solution $\bar{\mu}_{t/\lambda}(i)$ does not depend either on the value of λ .

Remark 4.6. Let $\bar{u}_t = \sum_i \bar{\mu}_t(i)$ be the proportion of unexplored nodes at time t and $P_t(CTS)$, the probability of receiving a CTS at time t (in the present case $P_t(CTS) = 1 - \bar{\alpha}_t(0)$). We may re-write Eq. (11) as

$$\theta = \lambda \int_0^\infty \bar{u}_t P_t(CTS) dt. \quad (12)$$

We will further discuss this alternative formulation in Sec. 5.2. Moreover, please note that if the probability of collision (or any other impairment) is not negligible as we assumed, it may be included in $P_t(CTS)$. Such extension is left for future work.

5. TRANSMISSION PROBABILITY OVER DIFFERENT INTERFERENCE GRAPHS

In this Section, we first look at the accuracy of the approximation of the transmission probability on configuration models with a finite number of nodes. Later on, we show how this methodology may be efficiently used to estimate the transmission probability of more complicated interference graphs stemming from spatial models.

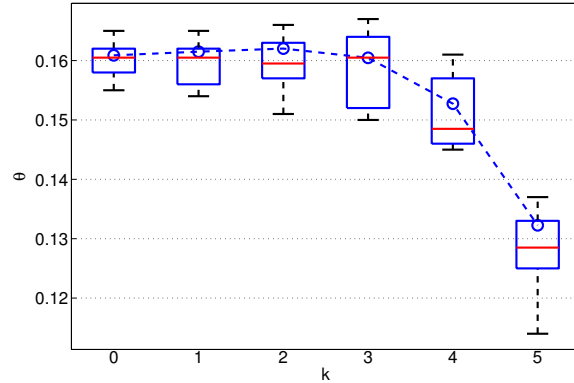


Fig. 3. The evaluation of Eq. (11) along with the boxplot of the numerical results of 10 simulations for $N = 1000$. The initial nodes' degree is uniformly distributed between $5 - k$ and $5 + k$, where k is indicated in the abscissa.

5.1. Configuration model with a uniform distribution

As a first illustration of the accuracy of Eq. (11) for finite large N , consider the example in Fig. 2. More precisely, we suppose that each node in the network has a number of neighbors ranging from $5 - k$ to $5 + k$ (with k varying between 0 and 5), all with the same probability. Figure 3 compares the limiting value θ (obtained from the solution of the limiting differential equation) and the simulations of 10 contention periods (in the form of a boxplot) for $N = 1000$.

Equation (11) provides an excellent approximation to the mean of Θ . Please note that the mean number of neighbors of each node is always 5, independently of k , which may be regarded as a parameter that controls the variance of the initial degree distribution. Interestingly, note that for low values of k the transmission probability seems independent of k whereas as it reaches 5, this probability significantly decreases. **As intuition tells, this particular example illustrates that the transmission probability does not depend only on the mean of the degree distribution.**

5.2. Configuration model with Poisson distribution

Equation (12) shows that in order to calculate θ we actually need to determine \bar{u}_t (i.e. $\sum_j \bar{\mu}_t(i)$), $P_t(CTS)$, and then the integral of their product. Let us then write down the differential equation that governs \bar{u}_t by summing Eq. (9) over all $i \in \mathbb{N}$. It is easy to verify that this produces:

$$\frac{d}{dt} \bar{u}_t = -\lambda \bar{u}_t \left(\bar{\alpha}_t(0) + \sum_j j \bar{\alpha}_t(j) + (1 - \bar{\alpha}_t(0)) \sum_j j \bar{\beta}_t(j) \right). \quad (13)$$

Again, this amounts to the normalized transition rate at time t times the expected number of nodes that are removed from the set of the unexplored ones (again, at time t). If the graph is such that this expected value depends only on the *cardinality* of this set (i.e. \bar{u}_t), then we would have a much simpler task than solving the complete set of equations (9).

As an example of such graph, let us discuss the graph we mentioned in Sec. 3, where all we knew was ν , the mean number of neighbors of each node. In the configuration algorithm described before, consider the moment where a tagged node attempts to

transmit. The neighbors of this node will be chosen from the complete set of blocked or unexplored nodes, each one with probability ν/N . When N is large, the degree distribution towards unexplored nodes of this tagged node will then be Poisson with parameter $\nu\bar{u}_t$. That is to say:

$$\bar{\alpha}_t(i) = \frac{(\nu\bar{u}_t)^i}{i!} e^{-\nu\bar{u}_t}.$$

Taking into account that $\sum_j j\bar{\beta}_t(j) = \sum_j j^2\bar{\alpha}_t(j)/\sum_j j\bar{\alpha}_t(j) = 1 + \nu\bar{u}_t$, we have that Eq. (13) in this case may be written as:

$$\begin{aligned} \frac{d}{dt}\bar{u}_t &= -\lambda\bar{u}_t(e^{-\nu\bar{u}_t} + \nu\bar{u}_t + (1 - e^{-\nu\bar{u}_t})(1 + \nu\bar{u}_t)) \\ &= -\lambda\bar{u}_t(1 + 2\nu\bar{u}_t - e^{-\nu\bar{u}_t}\nu\bar{u}_t), \end{aligned} \quad (14)$$

and the transmission probability equals

$$\theta = \lambda \int_0^\infty (1 - e^{-\nu\bar{u}_t})\bar{u}_t dt, \quad (15)$$

where (\bar{u}_t) solves Eq. (14).

Hence when the degree distribution tends to a Poisson distribution, the limiting differential equation can be greatly simplified using the strong degree independence of the Erdős Rényi graph. We indeed showed in [Bermolen et al. 2013] that a state space collapse does happen in that case since the number of explored nodes is itself Markov.

Figure 4 shows the corresponding transmission probability for 100 contention periods (in the form of a boxplot) for different values of both ν and N , along with the estimation provided by Eq. (15). Some interesting conclusions may be drawn from these graphs.

Firstly, when N is large, the estimation is not only an excellent approximation to the connection probability, but the variance of Θ is very small. Secondly, as N decreases, and although the variance increases significantly, Eq. (15) still provides an excellent approximation. This is further illustrated by Fig. 5. Lastly, a comparison between Figs. 3 and 4 shows again that the performance does not depend only on the mean degree: the present example gives a transmission probability of roughly 0.1 for a mean $\nu = 5$ neighbors and a variance $\nu = 5$. This same variance would be obtained in the uniform case (shown in Fig. 3) with k between 3 and 4, which results in a probability of successful transmission of more than 0.15.

5.3. Comparison with connection probabilities on fixed graphs

We now discuss a scenario falling outside the scope of the initial assumptions to illustrate the efficiency of this method for a large class of models. Let us assume that the communication graph is not random, but fixed. Thus, we may calculate the empirical distribution of neighbors of the initial graph (i.e. μ_0) and calculate (11) by solving Eq. (9). Though our method would consider a graph which is chosen randomly among all graphs that comply with the initial degree distribution, instead of a fixed graph, the resulting performance indicators still give reasonable approximations in many cases.

As a toy example, consider a lattice where every node has exactly k neighbors. Figure 6 shows a portion of these graphs for $k = 2, 4$. The initial distribution in this case is $\mu_0(i) = \delta(i - k)$.

For $k = 4$, simulations indicate a probability of successful transmission of 0.17, whereas our estimate is 0.185. Note that in the case of $k = 2$, all random graphs

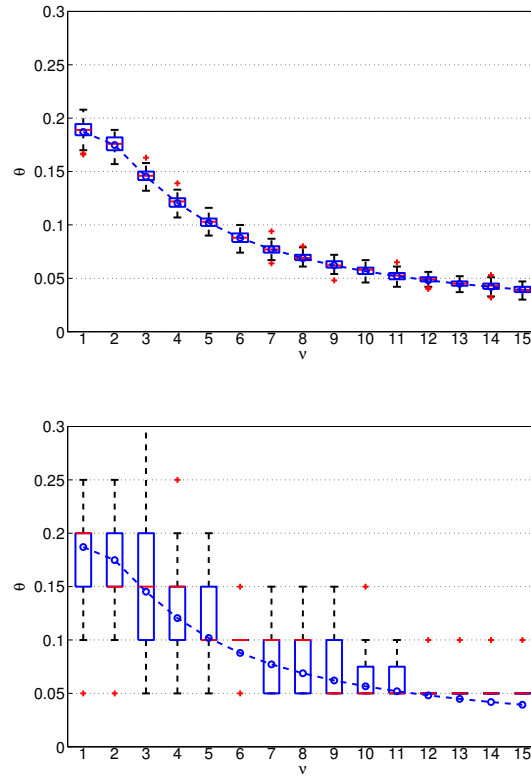


Fig. 4. The evaluation of Eq. (15) along with the boxplot of the numerical results of 100 simulations for $N = 1000$ (left) and $N = 20$ (right). The initial nodes' degree is distributed as a Poisson with parameter ν .

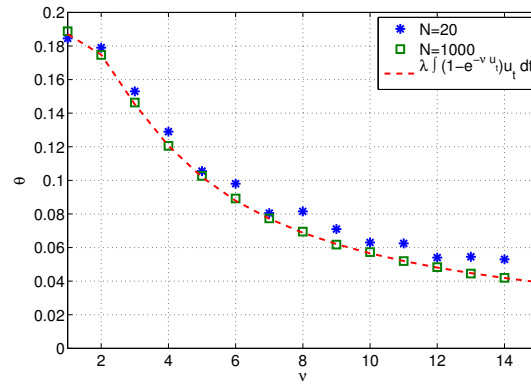


Fig. 5. The mean of the numerical results of 100 simulations for $N = 1000$ and $N = 20$, along with the evaluation of Eq. (15). The initial nodes' degree is distributed as a Poisson with parameter ν .

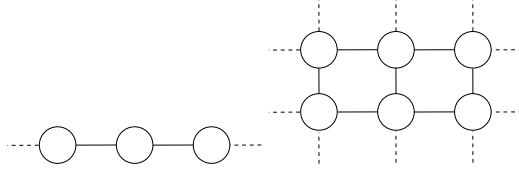


Fig. 6. The graph lattices considered: a line and a grid.

generated by $\delta(i - k)$ are either as in Fig. 6 or several circles of interconnected nodes. Since as N increases these circles include several nodes, our estimate is asymptotically exact.

5.4. Comparison with parking on a Poisson point process

As previously emphasized, our approach based on configuration models essentially ignores correlations between edges of the interference graph that are present when the graph stems from a spatial model. We numerically show here that this effect is quantitatively very small as soon as the interference graph has a sufficient amount of noise in the case of parking processes on a Poisson point process. Consider then the “classic” model where nodes are randomly and uniformly located in a plane. A transmission with power P of node s is received at node r with a *mean* power $P \times L(d_{sr})$, where d_{sr} is the distance between s and r , and $L(\cdot)$ is a monotonous decreasing function (generally termed *path loss*). This mean is taken over several time-slots. The receiving power during a given time-slot (which we will denote by $P(s, r)$) has random fluctuations around this mean, resulting in:

$$\frac{P(s, r)}{P} = L(d_{sr}) \times X_{sr},$$

where X_{sr} (generally termed *fading*) is a random variable with mean value equal to one.

Given a realization of the spatial process and the fading between every pair of nodes, the communication graph is constructed by including an edge between a pair of nodes s and r if $P(s, r) > P_{\min}$. The threshold P_{\min} is the sensitivity of the receiver, indicating the minimum power that it requires to correctly decode a frame. We will assume that fading is symmetrical, so that the resulting channels are also symmetrical.

As an example, consider a path-loss function $L(d) = d^{-a}$ (with $a = 2$) and log-normally distributed fading (whose logarithm is normally distributed with mean 0 and variance σ^2). Nodes will be positioned in the plane as in a Poisson process with intensity 1, and P/P_{\min} will be such that when $\sigma = 0$ the mean number of neighbors of each node will be $\nu = 2$ (i.e. $P/P_{\min} = (\pi/\nu)^{a/2}$).

Figure 7 shows the results corresponding to this scenario for different values of σ . Please note that $\sigma = 0$ corresponds to a variant of the so-called Matèrn hard core process [Stoyan and Stoyan 1985]. Just like in the previous example, in this case considering only the empirical degrees’ distribution results in a loss of information with an impact on the resulting performance. For instance, it is very likely that TX and RX have a neighbor in common. This in turn results in an underestimation of the probability of success, as shown in Fig. 7. However, as σ increases, this “spatial correlation” becomes weaker: the event of two nodes being neighbors is relatively less influenced by their distance. This results in increasingly more precise estimates of our method, which for a relatively small variance, $\sigma = 1$, already provides a very accurate estimate.

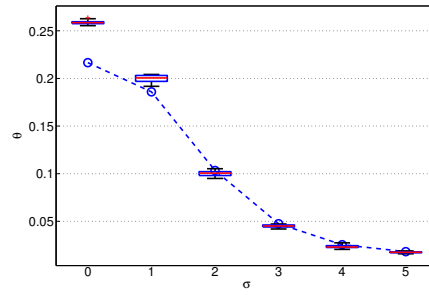


Fig. 7. The evaluation of Eq. (11) along with the boxplot of the numerical results of 10 time-slot simulations for a Poisson process with log-normal fading and a path-loss of the form $L(r) = r^{-2}$. The value of σ corresponds to the standard deviation of the underlying normal distribution.

6. MODEL EXTENSIONS

In the previous sections we have analyzed what we termed an ideal case, where the tagged node sends an RTS to every one of its neighbors until either one of them answers with a CTS or no more neighbors are left. Equivalently, this may be regarded as a situation where the tagged node's intended destination is always available. This could model for instance an opportunistic network where the actual destination of the RTS is any available node. If this is not the case, we have to analyze what happens when the RTS/CTS handshake fails.

In the following two subsections we briefly illustrate how our framework may be adapted with relative ease to study this scenario as well. More in particular, we will consider two possible situations when the tagged node is only interested in a single random neighbor. In the first one, if this node does not answer with a CTS, the neighbors of the tagged node (that overheard the RTS frame) will still be blocked for the rest of the contention period. In the second one, if this event occurs, the neighbors of the tagged node, realizing that the data transmission did not start, ignore the RTS and are not blocked by this failed handshake.

6.1. RTS/CTS handshake failure

Let us then consider the first scenario described above. For the sake of clarity, let us adapt the algorithm presented in Sec. 3.1 (which discussed how the *unexplored*, *active* and *blocked* set evolved over time) and highlight the differences with the ideal case. Assume we are in a transition time t_n when an unexplored node s sends an RTS frame. The first step is still to update the active and unexplored sets as follows:

$$\mathcal{A}_{t_n^+} \leftarrow \mathcal{A}_{t_n} \cup \{s\}; \quad \mathcal{U}_{t_n^+} \leftarrow \mathcal{U}_{t_n} \setminus \{s\}.$$

From the set \mathcal{N}_s of neighbors of s , we choose a random node r , if any. Then, we are in the following alternative:

- (1) If $r \notin \mathcal{U}_{t_n^+}$ (or $\mathcal{N}_s = \emptyset$), the scenario differs from above. The set of active nodes remains unchanged and we have to update the set of blocked nodes so as to include only the neighbors of s : $\mathcal{B}_{t_n^+} \leftarrow \mathcal{B}_{t_n} \cup \mathcal{N}_s$. The set of unexplored nodes is updated accordingly, i.e. $\mathcal{U}_{t_n^+} \leftarrow \mathcal{U}_{t_n^+} \setminus \mathcal{N}_s$. We then proceed to the next transmission attempt;
- (2) If $r \in \mathcal{U}_{t_n^+}$ we proceed exactly as before. That is to say, we include r among the active nodes ($\mathcal{A}_{t_n^+} \leftarrow \mathcal{A}_{t_n^+} \cup \{r\}$), update the blocked set of nodes ($\mathcal{B}_{t_n^+} \leftarrow \mathcal{B}_{t_n} \cup (\mathcal{N}_s \setminus$

$\{r\} \cup (\mathcal{N}_r \setminus \{s\})$) and the unexplored one ($\mathcal{U}_{t_n^+} \leftarrow \mathcal{U}_{t_n^+} \setminus (\mathcal{N}_s \cup \mathcal{N}_r)$). We then proceed to the next transmission attempt.

If we aim at a measure-valued representation of the system as above, it appears clearly that a state involving only the edges between unexplored nodes is not rich enough to obtain a Markov process. In particular, we now also need to track the number of blocked neighbors of the unexplored nodes, to calculate the probability of successfully completing the RTS/CTS handshake, which in turn defines the number of nodes that are removed from the measure, and their degree. We then introduce a bi-dimensional measure-valued process (μ_t) , where for any time t and any pair (i, j) of integers, $\mu_t(i, j)$ represents the number of unexplored nodes having i half-edges toward the unexplored set ($U \rightarrow U$ type), and j half-edges toward the blocked set ($U \rightarrow B$ type), at time t .

The initial measure is then defined as follows,

$$\mu_0(i, j) = \begin{cases} h(i) & \text{if } j = 0; \\ 0 & \text{if } j > 0, \end{cases}$$

that is to say, at $t = 0$ all nodes point towards unexplored nodes, and the measure is given by the nodes' degree distribution. Note that for any t , $\sum_j \mu_t(., j)$ yields the measure we had in the ideal case.

As we now demonstrate, the planar measure-valued process (μ_t) suffices to characterize the performance in the present case. For instance, and following the notation we used in Sec. 3.2, since TX is randomly chosen from all the unexplored nodes, at time t its degrees towards \mathcal{U}_t and \mathcal{B}_t have joint probability distribution given by

$$P(K_U^{\text{TX}} = i, K_B^{\text{TX}} = j) = \alpha_t(i, j) = \frac{\mu_t(i, j)}{\sum_{k,l} \mu_t(k, l)}, \quad i, j \in \mathbb{N},$$

where we added the subscripts U and B to indicate the type of half-edges, and where we omit, as above, the dependence on t for the sake of notational simplicity. Moreover, all the unexplored neighbors of an unexplored node (and in particular, RX) have the following degree distribution:

$$P(K_U^{\text{RX}} = i, K_B^{\text{RX}} = j) = \beta_t(i, j) = \frac{i\mu_t(i, j)}{\sum_{k,l} k\mu_t(k, l)}, \quad i, j \in \mathbb{N}.$$

As in the previous case, each step of the algorithm induces a modification on the process (μ_t) . If we scale it again, by considering $\bar{\mu}_t^N = \mu_t^N/N$ and take the limit when N goes to infinity we obtain a limit for the evolution of the process $(\bar{\mu}_t^N)$ which is a deterministic measure-valued function $(\bar{\mu}_t)$ which, as before, will be the solution of an infinite dimensional differential equation system. Following the discussion we presented for the ideal case, the right-hand of the equation for the evolution of $(\mu_t(i, j))$ for couples (i, j) , should be the mean number of nodes with i half-edges of type $U \rightarrow U$ and j half-edges of type $U \rightarrow B$ that are removed at time t , times the normalized total transition rate. The differential system thus results as follows: for all (i, j) ,

$$\begin{aligned} \frac{d}{dt} \bar{\mu}_t(i, j) = & -\lambda \sum_{k,l} \bar{\mu}_t(k, l) \left[\bar{\alpha}_t(i, j) + P_t(\text{CTS}^c) \mathbb{E}\{Y^{\text{TX}}(i, j) + X^{\text{TX}}(i, j) - X^{\text{TX}}(i+1, j-1) \mid \text{CTS}^c\} \right. \\ & \left. + P_t(\text{CTS}) \left(\bar{\beta}_t(i, j) + \mathbb{E}\{Y^{\text{TX,RX}}(i, j) + X^{\text{TX,RX}}(i, j) - X^{\text{TX,RX}}(i+1, j-1) \mid \text{CTS}\} \right) \right], \quad t \geq 0, \end{aligned} \tag{16}$$

where CTS refers here to the event described in step 2 above (i.e. the selected receiver is unexplored), and the superscript c refers to its complement. Thus we have that:

$$P_t(CTS) = \sum_{k,l} P_t(CTS | K_U^{\text{TX}} = k, K_B^{\text{TX}} = l) \bar{\alpha}_t(k, l) = \sum_{k,l} \frac{k}{k+l} \bar{\alpha}_t(k, l).$$

Please note that the main difference between Eqs. (16) and (10) lies in the definition of the event CTS and in the fact that TX blocks its neighbors even when this event does not occur (the second term between brackets).

The expected value of the rest of the random variables may be obtained analogously to how we proceeded before. For instance, the degree of the neighbors of TX ($Y^{\text{TX}}(i, j)$) follows a hypergeometric distribution with parameters K^{TX} and $\bar{\beta}_t(i, j)$. Then, the mean value of Y^{TX} results:

$$\mathbb{E}\{Y^{\text{TX}}(i, j) | CTS^c\} = \mathbb{E}\{K_U^{\text{TX}} | CTS^c\} \bar{\beta}_t(i, j).$$

Moreover, the number of nodes whose degree should be updated (the unexplored “neighbors of the neighbors”) are

$$Z^{\text{TX}} = \sum_{k>0, l} (k-1) Y^{\text{TX}}(k, l),$$

and we thus have that

$$\mathbb{E}\{X^{\text{TX}}(i, j) | CTS^c\} = \bar{\beta}_t(i, j) \sum_{k>0, l} (k-1) \mathbb{E}\{Y^{\text{TX}}(k, l) | CTS^c\}.$$

All in all, for all $t \geq 0$, Eq. (16) may be written in terms of $\bar{\mu}_t$, $\bar{\alpha}_t$ and $\bar{\beta}_t$ as follows:

$$\begin{aligned} \frac{d}{dt} \bar{\mu}_t(i, j) = & -\lambda \sum_{k,l} \bar{\mu}_t(k, l) \left[\bar{\alpha}_t(i, j) + \bar{\beta}_t(i, j) \sum_k k \bar{\alpha}_t(k) + \left(\sum_{k,l} \frac{k}{k+l} \bar{\alpha}_t(k, l) \right) \bar{\beta}_t(i, j) \left(\sum_{k>0, l} (k-1) \bar{\beta}_t(k, l) \right) \right. \\ & \left. + (\bar{\beta}_t(i, j) - \bar{\beta}_t(i+1, j-1)) \sum_{k>0, l} (k-1) \bar{\beta}_t(k, l) \left(\sum_{k,l} k \bar{\alpha}_t(k, l) + \left(\sum_{k,l} \frac{k}{k+l} \bar{\alpha}_t(k, l) \right) \left(\sum_{k>2, l} (k-2) \bar{\beta}_t(k, l) \right) \right) \right]. \end{aligned} \quad (17)$$

It should be clear that the same arguments as for the ideal case can be adopted to show the uniqueness of a solution $\bar{\mu}$ to (17), and numerically assess $\bar{\mu}$. We can then estimate the transmission probability as we did in Sec. 4.1, to obtain:

$$\mathbb{E}\{\Theta\} = \theta = \lambda \int_0^\infty \bar{u}_t P_t(CTS) dt = \lambda \int_0^\infty \sum_{k,l} \bar{\mu}_t(k, l) \sum_{k,l} \frac{k}{k+l} \bar{\alpha}_t(k, l) dt. \quad (18)$$

All the developments we presented in the previous sections also apply to this case. For instance, and as example of both the accuracy and the limitations of our approach, Fig. 8 shows the results for this case in the same scenario as in Sec. 5.4 (Poisson hard core process). Again, the information lost by considering only the initial nodes’ degree distribution may have a significant impact (small values of σ in this case). If this is not the case, our approach yields very precise results.

6.2. RTS/CTS handshake failure with timeout

Let us study the second scenario under a handshake failure. In the previous subsection, the neighbors of TX were blocked by the RTS and did not compete further for the

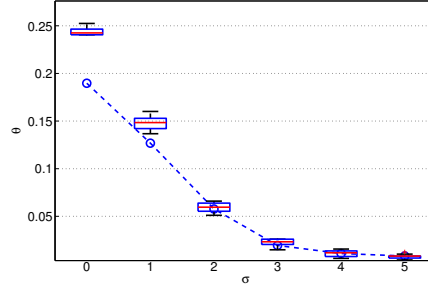


Fig. 8. The evaluation of Eq. (18) along with the boxplot of the numerical results of 10 time-slot simulations for a Poisson process with log-normal fading and a path-loss of the form $L(r) = r^{-2}$. The value of σ corresponds to the standard deviation of the underlying normal distribution.

channel, even if no data transmissions ensued. However, a time-out is generally implemented in this kind of access, where the RTS alone blocks the nodes during a certain time. If no further transmissions are sensed afterwards, the RTS is ignored and the node starts competing for the medium again. Let us then consider an idealization of this mechanism, where this realization is instantaneous. As we will discuss later, the presented extension is also capable of modeling a situation where the tagged node has no packets to send and acts only as a receiver.

Please note that in this case, nodes whose RTS frame went unanswered will in turn be able to answer with a CTS if a RTS frame is addressed to them. Thus, they belong neither to the blocked nor active set of nodes. In this section we define a new class of nodes: *sans*-CTS. We will say the node belongs to class S (and the corresponding set \mathcal{S}_t) if it is available only as a receiver (it has tried to communicate without success).

To highlight the differences with the previous scenario, we discuss here the different possibilities that arise when an unexplored node s tries to communicate with a randomly selected neighbor at time t_n . The first step this time is to update only the set of unexplored nodes $\mathcal{U}_{t_n}^+ \leftarrow \mathcal{U}_{t_n} \setminus \{s\}$. Once we have chosen a random neighbor of s ($r \in \mathcal{N}_s$), the following two cases are possible:

- (1) If $r \notin \mathcal{U}_{t_n}^+ \cup \mathcal{S}_{t_n}$ was chosen (or if $\mathcal{N}_s = \emptyset$), the set of active nodes remains unchanged. Moreover, the node s is still available as a receiver and its neighbors are not blocked. That is to say, $\mathcal{S}_{t_n}^+ \leftarrow \mathcal{S}_{t_n} \cup \{s\}$ and we proceed to the next transmission attempt.
- (2) If $r \in \mathcal{U}_{t_n}^+ \cup \mathcal{S}_{t_n}$ was chosen (i.e. the neighbor is unexplored or available), we further update the sets as before, including s in the active set: $\mathcal{A}_{t_n}^+ \leftarrow \mathcal{A}_{t_n} \cup \{s, r\}$, $\mathcal{B}_{t_n}^+ \leftarrow \mathcal{B}_{t_n} \cup (\mathcal{N}_s \setminus \{r\}) \cup (\mathcal{N}_r \setminus \{s\})$ and $\mathcal{U}_{t_n}^+ \leftarrow \mathcal{U}_{t_n}^+ \setminus (\mathcal{N}_s \cup \mathcal{N}_r)$. Moreover, the involved nodes that belonged to \mathcal{S}_{t_n} should be removed from it: $\mathcal{S}_{t_n}^+ \leftarrow \mathcal{S}_{t_n} \setminus (\mathcal{N}_s \cup \mathcal{N}_r)$. We then proceed to the next transmission attempt.

The measure-valued Markov process approach is more involved in this scenario. To begin with, we need to define at each time t , a three-dimensional measure $\mu_t(i, j, k)$ to keep track of the degree of a given unexplored node towards the unexplored, blocked and *sans*-CTS nodes. Moreover, we also need the information about the degree of the *sans*-CTS nodes towards the unexplored and *sans*-CTS sets. This is necessary since, for instance, once a node is chosen as a receiver, it will block its unexplored neighbors. This receiver may belong either to \mathcal{U}_t or \mathcal{S}_t .

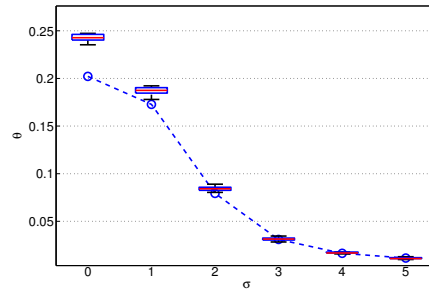


Fig. 9. The evaluation of Eq. (19) along with the boxplot of the numerical results of 10 time-slot simulations for a Poisson process with log-normal fading and a path-loss of the form $L(r) = r^{-2}$. The value of σ corresponds to the standard deviation of the underlying normal distribution.

In brief, at time t we need two measures, $\mu_t(i, j, k)$ and $\nu_t(i, j)$. The measure $\mu_t(i, j, k)$ represents the number of unexplored nodes with i half-edges toward the unexplored set ($U \rightarrow U$ type), j half-edges toward the blocked set ($U \rightarrow B$ type) and k half-edges toward the *sans*-CTS set ($U \rightarrow S$ type). Analogously, $\nu_t(i, k)$ represents the number of *sans*-CTS nodes with i half-edges toward the unexplored set ($S \rightarrow U$ type) and k half-edges towards the *sans*-CTS set ($S \rightarrow S$ type). At time $t = 0$ these measures are:

$$\mu_0(i, j, k) = \begin{cases} h(i) & \text{if } j = k = 0, \\ 0 & \text{if } j, k > 0, \end{cases} \quad \text{and} \quad \nu_0(i, k) = 0,$$

that is, initially all nodes are unexplored and point towards unexplored nodes. Please note that the half edges of type $S \rightarrow B$ do not matter since S nodes act only as receivers (as opposed to $U \rightarrow B$ half-edges, which are required to calculate $P_t(CTS)$). In this sense, we could analyze a situation where some nodes are deployed as receivers only, by assigning them to the initial measure ν_0 (and reflecting this on μ_0).

We then analyze a large graph limit when the number of nodes goes to infinity as we did for the previous cases. The procedure is essentially the same: to write down the evolution of $(\mu_t(i, j, k))$ (respectively $(\nu_t(i, j))$), we identify at each step of the algorithm the mean number of nodes of each type and degree that should be removed from the measure. The random variables we defined before (notably Y and X) have to be adapted to this case, but their distribution is essentially the same. For the sake of clarity, and since our objective here is to illustrate possible extensions of our framework, we do not write the differential equation systems.

Once we have obtained a (numerical) solution of the latter, we can estimate as before the probability of a successful transmission as:

$$\mathbb{E}\{\Theta\} = \theta = \lambda \int_0^\infty \bar{u}_t P_t(CTS) dt, \quad (19)$$

where for all $t \geq 0$, $\bar{u}_t = \sum_{i,j,k} \bar{\mu}_t(i, j, k)$, $P_t(CTS) = \sum_{i,j,k} \frac{i+k}{i+j+k} \bar{\alpha}_t(i, j, k)$ and $\bar{\alpha}_t$ is defined as before.

Again, and for illustrative purposes, we consider the example of the Poisson hard core process. The results, presented in Fig. 9, again show that when the initial nodes' degree distribution is enough to describe the statistics of the resulting communication graph (corresponding to the higher values of σ), then our method yields very accurate estimates.

7. CONCLUSIONS AND FUTURE WORKS

We showed how stochastic dynamics on configuration models can provide powerful performance tools for quantifying the effect of interference on the performance of wireless networks. Through extensive simulations we have shown under which circumstances the method yields accurate results. In a nutshell, this is so when neighboring nodes are not likely to share neighbors between them (for instance, in the presence of fading). Since this is not always the case, error bounds and stochastic comparison results for spatial models are future research directions of great practical importance.

Another interesting future research line concerns the channel model we considered. As data rates increase (for instance, those used in the actual data transmissions), interference may become the decisive factor in determining the correct reception of transmissions. This means for instance that a node may seize the channel during the RTS/CTS exchange, but its data transmission may fail due to the summed interference of other concurrent transmissions in the receiving node. The analysis of this second stage and its inclusion in our framework is indeed a challenging task which deserves further research.

Finally, it would be interesting to verify whether the proposed methodology may be adapted to other MAC mechanisms. For example, Aloha is used in Wireless Sensor Networks for certain specific tasks such as neighbor discovery or information propagation. This adaptation is not trivial, since this new context significantly differs from the one considered here. For instance, in the case of information propagation, traffic is not saturated and we would be interested in how much time elapses until a certain information is shared among all nodes.

REFERENCES

- François Baccelli and Bartłomiej Błaszczyszyn. 2009a. Stochastic Geometry and Wireless Networks, Volume 1: Theory. *Foundations and Trends in Networking* 3, 3-4 (2009), 249–449. DOI: <http://dx.doi.org/10.1561/1300000006>
- François Baccelli and Bartłomiej Błaszczyszyn. 2009b. Stochastic Geometry and Wireless Networks, Volume 2: Applications. *Foundations and Trends in Networking* 4, 1-2 (2009), 1–312. DOI: <http://dx.doi.org/10.1561/1300000026>
- Paola Bermolen, Matthieu Jonckheere, and Pascal Moyal. 2013. The Jamming Constant of Random Graphs. (2013). <http://arxiv.org/abs/1310.8475> Submitted.
- G. Bianchi. 2000. Performance Analysis of the IEEE 802.11 Distributed Coordination Function. *IEEE J. Sel. A. Commun.* 18, 3 (September 2000), 535–547. DOI: <http://dx.doi.org/10.1109/49.840210>
- B. Bollobas. 2001. *Random Graphs*. Cambridge University Press, Cambridge, UK.
- Charles Bordenave, David McDonald, and Alexandre Proutiere. 2012. Asymptotic Stability Region of Slotted Aloha. *IEEE Transactions on Information Theory* 58, 9 (2012), 5841–5855. DOI: <http://dx.doi.org/10.1109/TIT.2012.2201333>
- S.C. Borst, M. Jonckheere, and L. Leskelä. 2008. Stability of parallel queueing systems with coupled service rates. *Discrete Event Dyn. Syst.* 18, 4 (2008), 447–472.
- Pierre Bremaud. 1999. *Markov Chains: Gibbs Fields, Monte Carlo Simulation, and Queues*. Springer, New York, USA.
- F. Cecchi, S.C. Borst, and J.S.H. van Leeuwen. 2014. Throughput of CSMA networks with buffer dynamics. *Performance Evaluation* 79, 0 (2014), 216 – 234. DOI: <http://dx.doi.org/10.1016/j.peva.2014.07.014> Special Issue: Performance 2014.
- Dawson D.A. 1991. *Measure-Valued Processes, Stochastic Partial Differential Equations, and Interacting Systems*. Vol. 5. American Mathematical Society, Rhode Island, USA.
- R. Durrett. 2007. *Random graph dynamics*. Cambridge University Press, Cambridge, UK.
- M. Durvy and P. Thiran. 2006. A Packing Approach to Compare Slotted and Non-Slotted Medium Access Control. In *INFOCOM 2006. 25th IEEE International Conference on Computer Communications. Proceedings*. IEEE, Barcelona, Spain, 1–12. DOI: <http://dx.doi.org/10.1109/INFCOM.2006.251>
- Dave Evans. 2011. *The Internet of Things: How the Next Evolution of the Internet Is Changing Everything*. Technical Report. Cisco. http://www.cisco.com/web/about/ac79/docs/innov/IoT_IBSG_0411FINAL.pdf

- P. Gupta and P.R. Kumar. 2000. The capacity of wireless networks. *Information Theory, IEEE Transactions on* 46, 2 (Mar 2000), 388–404.
- IEEE. 2012. 802.11-2012 - IEEE Standard for Information technology–Telecommunications and information exchange between systems Local and metropolitan area networks–Specific requirements Part 11: Wireless LAN Medium Access Control (MAC) and Physical Layer (PHY) Specifications. (2012).
- Federico Larroca and Fernanda Rodriguez. 2014. An Overview of WLAN Performance, Some Important Case-Scenarios and Their Associated Models. *Wireless Personal Communications* 79, 1 (2014), 1–54.
- M. Molloy and B. Reed. 1995. A critical point for random graphs with a given degree sequence. *Random structures and algorithms* 6 (1995), 161–180.
- H.Q. Nguyen, F. Baccelli, and D. Kofman. 2007. A Stochastic Geometry Analysis of Dense IEEE 802.11 Networks. In *26th IEEE International Conference on Computer Communications. INFOCOM 2007*. IEEE, Anchorage, USA, 1199–1207.
- M D Penrose. 2001. Random parking, sequential adsorption, and the jamming limit. *Commun. in Math. Phys.* 218, 1 (2001), 153–176.
- M D Penrose and A Sudbury. 2005. Exact and approximate results for deposition and annihilation processes on graphs. *Annals of Applied Probability* 15, 1B (2005), 853–889.
- Dietrich Stoyan and Helga Stoyan. 1985. On One of Matérn’s Hard-core Point Process Models. *Mathematische Nachrichten* 122, 1 (1985), 205–214.
- Wojciech Szpankowski. 1983. Packet Switching in Multiple Radio Channels: Analysis and Stability of a Random Access System. *Computer Networks* 7 (1983), 17–26. DOI: [http://dx.doi.org/10.1016/0376-5075\(83\)90004-1](http://dx.doi.org/10.1016/0376-5075(83)90004-1)
- Remco van der Hofstad. 2013. Random Graphs and Complex Networks. (2013). Lecture Notes.
- Nguyen Tien Viet and François Baccelli. 2012a. Generating Functionals of Random Packing Point Processes: From Hard-Core to Carrier Sensing. (2012). <http://arxiv.org/abs/1202.0225>
- Nguyen Tien Viet and François Baccelli. 2012b. On the spatial modeling of wireless networks by random packing models. In *Proceedings of the IEEE INFOCOM 2012*. IEEE, Orlando, USA, 28–36. DOI: <http://dx.doi.org/10.1109/INFCOM.2012.6195725>
- Nicholas C Wormald. 1995. Differential equations for random processes and random graphs. *The annals of applied probability* 5, 4 (1995), 1217–1235.
- Nicholas C Wormald. 1999. *Models of random regular graphs*. Cambridge University Press, Cambridge, UK, 239–298.